Electron Impact Ionization of 1-Butanol: II. Total Ionization Cross Sections and Appearance Energies

S. Ghosh[1], K. L. Nixon[1,2], W. A. D. Pires[1], R. A. A. Amorim, R. F. C. Neves[1,3], H. V. Duque[1], D. G. M. da Silva[1], D. B. Jones[4], F. Blanco[5], G. Garcia[6], M. J. Brunger[4] and M. C. A. Lopes[1] *

[1] Departamento de Física, Universidade Federal de Juiz de Fora, Juiz de Fora, MG, 36936-900, Brazil
[2] School of Sciences, University of Wolverhampton, Wolverhampton WV1 1LY, UK
[3] Instituto Federal do Sul de Minas Gerais, Campus Poços de Caldas, Minas Gerais, Brazil
[4] College of Science and Engineering, Flinders University, GPO Box 2100, Adelaide SA 5001, Australia
[5]Departamento de Fisica Atomica, Molecular y Nuclear, Universidad Complutense de Madrid, 28040 Madrid, Spain
[6] Instituto de Fisica Fundamental, Consejo Superior de Investigaciones Cientiíficas (CSIC), Serrano 113-bis, 28006 Madrid, Spain

* corresponding author: cristina.lopes@ufjf.edu.br

Abstract

Experimental and theoretical data on total ionization cross sections for electron scattering by 1-butanol molecules in the energy range 10-100 eV are reported in this work. The experimental data were obtained from the addition of partial ionization cross sections (PICS) of 38 cationic fragments registered using a Hiden Analytical quadrupole mass spectrometer (EPIC 300), which are reported in a companion paper (Pires *et al*., 2018). The theoretical data were generated using the Binary-Encounter-Bethe and independent atom model plus screening corrected additivity rule approaches. Additionally, we also reported the appearance energies (AEs) and Wannier exponents for 36 of the 38 main cationic fragments observed in our experiments. Our experimental TICS data are typically found to be in good agreement with our theoretical results, and with other experimental and theoretical TICS data of 1-butanol currently available in the literature. Agreement of our AEs and the previous data, again where a comparison is possible, is also found to be satisfactory.

PACS numbers: 34.80.Ht, 34.80.Gs

1. Introduction

Electron impact ionization of molecules is relevant to a wide range of applications [1], including plasmas, atmospheric science, magnetic fusion, radiation physics and astrophysics (e.g. [2-5]). In addition to these applications, the electron impact ionization of the primary alcohols is very significant due to the possibility of those alcohols being used as a biofuel in combustion engines. There are many advantages of using these alcohols to replace fossil fuels, as for a prompt example, we note that primary alcohols are cheaper and their combustion is less polluting than oil derivates [6]. In this context, electron impact ionization cross sections provide important information about the electron-fuel interactions occurring during spark ignition [7], given that those data helps in understanding the mechanisms for the maximum energy release during the combustion process. In spite of the relevance pointed out, to date, while there have been significant theoretical and experimental studies into the electron impact ionization for smaller primary alcohols such as methanol, ethanol, and 1-propanol, the investigations for larger molecules such as 1-butanol still remain very scarce [5].

Ethanol, nowadays the most well-known and used biofuel, is not an ideal fuel due to its lower energy density than gasoline, and its hygroscopic nature which presents a problem for storage and distribution. 1-Butanol, on the other hand, is a superior fuel compared to ethanol [8], since it contains a low oxygen content (22%), that leads to a cleaner burn. Further, the fact that it possesses a longer carbon chain [9,10], gives it a higher energy density than that of gasoline, and also makes it less volatile than ethanol. 1-Butanol, having a higher motor octane rating (94) and higher energy content (110,000 BTUs / gallon) compared to ethanol (motor octane 92, energy content 84,000 BTUs / gallon) releases greater energy during the internal combustion process. Furthermore, its low vapor pressure makes it combustible but not flammable. This results in Butanol being a potentially safer fuel to use compared to methanol, ethanol and gasoline, which are all flammable and potentially explosive.

Electron impact ionization of atoms and molecules has been studied for the last 90 or so years, and there have been many theories developed, based on the classical model of electron collisions, and also first principle theories to account for the total ionization cross section due to electron impact. Traditionally, electron collisions are divided into two categories, namely soft collisions which involve long-range large impact parameter interactions and hard collisions which involve short range collisions at small impact parameters. The Mott theory [11], one of the oldest theories proposed to deal with this problem, cannot accurately describe the soft collision between two electrons. An important work was introduced by Bethe in 1930 [12], by using the plane-wave Born approximation (PWBA) [13] to determine an accurate form of the ionization cross section for high energy collisions for a wide range of molecules, large and small, including radicals and positive ions. In 1994 Kim and Rudd [14] introduced the Binary-Encounter-Bethe (BEB) model, by combining binary encounter theory with the dipole interactions of the Bethe theory, for fast inelastically scattered electrons. Nowadays, there are many studies that have applied the BEB theory [15-17], modified BEB theory [18,19] and relativistic BEB theory [20], to estimate the total ionization cross section due to electron impact. An excellent recent summary of those endeavours can be found in Tanaka *et al*. [21]. Deutsch and Märk (DM) introduced a different approach, known as the DM formalism [22-25], by combining the Born-Bethe approximation and the additivity rule to calculate absolute electron impact ionization cross sections for technologically relevant molecules. There are several other theoretical models employed to investigate the total electron impact ionization cross sections, including the spherical complex

optical potential formalism [26-28] and the independent atom model with screening corrected additivity rule (IAM-SCAR) [29,30]. In this investigation, TICS for 1-butanol were calculated within the BEB formalism and the IAM –SCAR method [31, 32], the latter as widely described in our previous papers [31, 32].

From the experimental perspective, in terms of studies for electron-atom (or molecule) collisions have been performed using several different experimental techniques over the years in order to obtain electron-impact ionization cross sections. For example, Rapp and Englander-Golden [33] reported the total ionization cross section of various molecules from threshold to 1000 eV in a total ionization tube. Additionally, Srivastava *et al.* [34-36] used a crossed electron-beam-molecular-beam, with a relative flow normalization technique, to estimate the partial and total ionization cross sections of a wide range of molecules. Furthermore, Nishimura *et al.* [37] reported TICS for a range of hydrocarbons by employing a parallel plate ion collector method with a magnetically confined linear electron beam. Finally, Straub *et al.* [38-41] estimated partial ionization cross sections for various molecules by using a time-of-flight mass spectrometer. Of particular relevance to this investigation, we note that there has also been a number of studies about the electron impact total and partial ionization cross sections, and ionic fragment appearance energies, of methanol [42-48], ethanol [43, 44, 46, 48] and 1-propanol [43, 44, 49, 50]. Indeed our group has also studied electron impact ionization and fragmentation, absolute total and partial ionization cross sections, and appearance energies of methanol [51, 52], ethanol [51, 52] and 1-propanol [53, 54]. Hence the current 1-butanol investigation can be considered to be an extension of those previous works [51-54].

There are some important earlier studies about the electron impact ionization of 1-butanol. For instance, Freidel *et al.* [55] reported the mass spectra of 69 alcohols including 1-butanol, while Zavilopulo *et al.* [48] studied the dissociative ionization of 1-butanol by using the crossed electron and molecular beam method with the help of a monopole mass spectrometer. Further, they have studied the relative ionization cross sections of the ionic fragments from 5eV to 60 eV. Hudson *et al.* [44] studied the total electron impact ionization cross section and the ionization potentials of the butanol isomers from threshold to over a 200 eV energy range. The BEB results reported in their work were later found to be in error, consequently being updated by Bull *et al*. [49]. From the applied point of view, Oßwald et al. [56] developed an investigation of the combustion for the isomers of 1-butanol by using a molecular beam mass spectrometry (MBMS) technique, while Weber and Sung [57] reported an interesting study about the comparative auto-ignition trends in the butanol isomers at elevated pressure.

The structure of the remainder of this manuscript is as follows. The experimental methods, analysis procedures and theoretical details are given in Section 2, while our total ionization cross sections, both theory and experiment, and appearance energy results are presented and discussed in Section 3. Note that we believe that the current 1-butanol appearance energy investigation is the most comprehensive to date. Finally, some conclusions from this work are detailed in Section 4.

2. Experimental Methods, Data Analysis and Theoretical Details

The current experimental procedure is similar to that described in detail in our previous work [52, 54], and in our companion paper to this one [58]. Hence while some details are repeated, this cannot be avoided as we wish the present paper to be as self-

contained as possible. Our experiments were carried out using a Hiden Analytical system which is composed of a mass spectrometer interface unit (MSIU), a radio frequency (RF) head, and an EPIC 300 probe. The EPIC 300 probe utilizes a quadrupole mass spectrometer (QMS) to filter the cations based on their mass-to-charge (m/z) ratio. The QMS is housed within a vacuum chamber, which is evacuated by a turbo molecular pump backed by a dry scroll pump. Here, the chamber typically has a base pressure of ~ 2.1 x 10^{-7} torr, with the actual measurements being performed using an operating pressure of ~ 1.5 x 10^{-6} torr. The sample of liquid 1-butanol, purified by several freeze-pump-thaw cycles, was introduced in the gas phase by effusion into the ionization chamber though a capillary needle. The vapour pressure of 1-butanol at the laboratory temperature (22°C) was approximately 5.32 torr, as calculated using the Antoine equation [59]. Thermionic electrons from an yttria-coated iridium filament were accelerated to the desired energy and then used as an internal ionization source to create ions by electron impact. During the measurements, the incident electron current in the ionizer was 20 μA and the electron energy spread was about 660 meV [54]. The present spectrometer has been optimized and calibrated through measuring the PICS for argon, Ar^+, over the energy range from 10-100 eV, with our values benchmarked against those of Rejoub *et al.* [43]. Our measurements on 1-butanol were carried out on several separate days spanning the course of the investigation. In the present work, the MSIU enables a mass spectrum to be obtained by recording the count rate of the ions at a fixed incident electron energy while scanning over the mass range of interest. Alternatively, the ion signal at a particular mass is monitored while scanning over a range of incident electron energies. Here, the operation and data recorded with the MSIU is controlled through a PC user interface. Finally, the background signal was subtracted from the main signal in order to obtain accurate values for the PICS [58]. A full discussion of the PICS is provided in our companion paper [58]. While we in fact measure a mass to charge ratio in the experiment, all fragments detected are expected to be singly charged, and so we explicitly refer to these by their mass specific fragments (in amu). An explanation justifying this rationale is found in Pires *et al.* [58]. The total ionization cross section (TICS) is obtained by summing up the contribution of all ion signals observed at each incident electron energy. Note that the absolute values of our TICS and PICS were obtained through the normalization of our data at 70 eV, to the absolute value of the 1-butanol TICS reported by Hudson *et al.* [44] as obtained using an ionization cell.

Experimental determination of the appearance energies, for the observed ion fragments produced in ionization processes near to their onset threshold, is a difficult task because of their low ion signal rates. For the last few decades, some experimentalists have used mass spectrometry to determine the appearance energies and ionization energies [60-63] of various ions and ion fragments. There are many theoretical models that attempt to explain the near-threshold energy behaviour of an atom, for single and multiple ionization processes of atoms and molecules. One of the most widely accepted models, although it is semi-classical in its construction, is the Wannier law [64], applicable for a small but finite energy range above the ionization threshold. The Wannier type function [65], the so-called p^{th} power law, has been proposed for fitting the experimental partial ionization data in the threshold region, to determine the appearance energy. Here the Wannier type function, with $\sigma(E)$ as the cross section, can be written as follows [65]:

$$\sigma(\mathrm{E}) = \begin{matrix} 0 & \mathrm{E} < \mathrm{AE} \\ \mathrm{A}(\mathrm{E}-\mathrm{AE})^{\mathrm{p}} & \mathrm{E} \geq \mathrm{AE} \end{matrix} . \qquad (1)$$

The appearance energies (AE) can thus, in principle, be determined from the Wannier law, by fitting the relevant cation intensity data of counts verses impact energy, E, at energies near to the threshold. However, to obtain an accurate value of the appearance energy the

finite energy resolution of the incident electron beam needs to be accounted for. Märk et al. [66-68] thus proposed to employ a nonlinear fitting of the Wannier threshold law, after its convolution with a Gaussian function to represent the energy spread of the incident electron beam. Namely, the measured ion yield f(E) is given by:

$$f(E) = \int_{AE}^{\infty} \frac{-(E-E_0)^2}{2\sigma^2} [A(E_0 - AE)^p] dE_0. \qquad (2)$$

Here A is a scaling factor, p is the Wannier exponent, and now σ is related to the energy spread [full-width-half-maximum (FWHM)] of the incident electron beam. The non-linear fitting was performed using a Marquart-Levenberg algorithm implemented in the Origin 2016 package. Note that the above procedure is identical to that used in our recent work [54]. If we were to use equation 1, instead of equation 2, for the experimental data fitting, then the resultant fits give slightly higher values of the appearance energy, as shown in ref [69]. The appearance energy of argon (15.759 eV) [66] was used to calibrate the energy scale. Furthermore by performing the fit to the argon-ion yield with the well-established Wannier exponent for argon, i.e. with p = 1.35 [66], we obtained a value of σ = 0.28 eV, which gives the energy resolution of the incident electron beam as ~660 meV. This value of σ was then fixed for the subsequent analysis of all the 1-butanol data, with representative results from this analysis procedure being shown in figure 1. The ion counts for each fragment were measured in 0.1 eV steps in the region of the appearance energy. This was done for both the background vacuum and once the 1-butanol had been admitted. The background data was subsequently subtracted from the signal data. By fitting the 1-butanol relative PICS within the energy range around the AE threshold, we have performed the nonlinear fit and obtained the appearance energies for 36 of the most prominent cations formed in the ionization of 1-butanol. These values are detailed in table 1. The fitting of the onset ionization threshold curves was performed for ± 3eV and ± 2eV range around the AE observed visually, ultimately choosing the result that presented the best fit, and therefore a smaller error. In some cases, it was observed that the fitting for the ± 3 eV range had a smaller error. If in both analyses of the ion yield curve (using ± 3eV and ± 2eV), it was not possible to reproduce satisfactorily the experimental onset threshold, a new fitting with two AEs was considered. That is, reflecting the formation of the cation studied through two distinct dissociation processes. The fitting of the ion yield curve for CH_3^+ in figure 1 illustrates this procedure, where adjustment of two AEs was required for the 15 a.m.u. of 1-butanol. In this fitting, the total energy range considered was 8.4 -20.0 eV. It was found that the first AE_1 = 10.16 eV and the second AE_2 = 14.56 eV. This procedure to determine two AEs for a single mass value, involving two distinct dissociation processes, was also used in our previous study of 1-propanol [54].

To supplement our experimental work, theoretical calculations for the total ionization cross section are obtained within the Binary Encounter Bethe (BEB) and independent atom model – screening corrected additivity rule (IAM-SCAR) frameworks. At the BEB level of approximation [14, 21], the total ionization cross section, Q_{ion}, is obtained by summing up the partial ionization cross sections over the N-occupied 1-butanol orbitals:

$$Q_{ion}(E_0) = \sum_{i=1}^{N} Q_i(t_i) \quad . \qquad (3)$$

Here the contribution from the i^{th} molecular orbital, Q_i, to the total ionization cross section is obtained via:

$$Q_i(t_i) = \frac{4\pi a_0^2 N_i (R/B_i)^2}{t_i + u_i + 1}\left[\frac{\ln(t_i)}{2}\left(1 - \frac{1}{t_i^2}\right) + 1 - \frac{1}{t_i} - \frac{\ln(t_i)}{t_i + 1}\right], \quad (4)$$

where $t_i = E_0/B_i$ and $u_i = U_i/B_i$, with a_0 and R being the Bohr radius and the Rydberg energy, respectively. N_i, B_i and U_i are the ionized orbital's occupation number, bound state binding energy and average orbital electron kinetic energy, respectively. In our implementation of the BEB formulation, the geometry of 1-butanol was optimized at the B3LYP/aug-cc-pVDZ level for the most abundant trans-trans, gauche-trans and trans-gauche conformers [70]. Butanol has a ground electronic-state with configuration,

$$X^1A\text{: } \underbrace{(1a)^2\ (2a)^2\ \ldots\ (5a)^2}_{Core}\ \underbrace{(6a)^2\ (7a)^2\ \ldots (21a)^2}_{Valence}.$$

Single point energy calculations were performed for each conformer at the optimised geometry, at the density functional theory (B3LYP/aug-cc-pVDZ) level, to derive the necessary average orbital kinetic energies required to implement the BEB calculation. Here we also performed outer-valence Green's function level, OVGF/aug-cc-pVDZ, calculations to obtain orbital ionization energies, although in practice we ultimately used experimental photoelectron values for the outer valence orbital binding energies (B_i). These values were supplemented with those obtained at a Koopman's theorem level for ionization of the inner valence orbitals, after applying a linear correction factor derived using the outer valence values. BEB cross sections are often calculated using the OVGF formalism, however, the OVGF calculation is performed using canonical Hartree-Fock orbitals that do not include dynamic electron correlation effects. We have therefore also calculated the BEB cross section values with this OVGF type approximation. The BEB cross sections for each conformer typically agree to within 1% of each other, except near the ionization threshold where differences of 3% may be observed. These differences are within the expected uncertainty of the BEB formalism. As such, the BEB total ionization cross section at the OVGF and B3LYP levels are only reported for the lowest energy gauche-trans conformer [70].

The independent atom model – screening corrected additivity rule (IAM-SCAR) framework is a self-consistent framework for describing a range of scattering processes. Here the cross sections are derived by considering the sum of individual electron scattering processes from each individual atom present within the target molecule, with a screening correction derived from the target molecule's geometry implemented to describe the interactions between individual atoms within the molecule. The electron scattering cross sections for a particular atom are obtained using an optical model based on a potential scattering approach. Here the local complex potential is given by,

$$V(r) = V_s(r) + V_{ex}(r) + V_p(r) + iV_a(r). \quad (5)$$

In equation 5 $V_s(r)$ is the Hartree-Fock potential of the target [71], $V_{ex}(r)$ is the electron exchange interaction [72], $V_p(r)$ is the dipole polarization [73] and $iV_a(r)$ is the complex absorption potential [74]. The imaginary nature of the potential yields complex phase shifts, that can be used to calculate differential and integral cross sections for elastic

and inelastic scattering processes. The IAM-SCAR formalism can be implemented with an energy dependent absorption energy threshold, to allow for the separation of the ionization and discrete inelastic absorption channels [75]. In this way, we can obtain a total ionization cross section within the IAM-SCAR framework. We note that the present IAM-SCAR approach also includes interference effects [76], although they do not affect the absorption cross sections obtained at the IAM-SCAR level of approximation.

3. Result and discussion

3.1 Appearance Energies

Figure 1 shows typical examples of the fitting of the ion yield experimental data (or relative partial ionization cross sections) for 4 cationic fragments of 1-butanol. The appearance energies and Wannier exponents obtained for the 36 most intense cations, within the mass spectrum, are listed in table 1, along with those reported within the NIST database where available [77]. The NIST database only contains appearance energies for 4 cations (74, 56, 42, 31 amu) of 1-butanol, with the present data for these cations being in pretty good accord with those reported values.

In our dataset shown in the table 1, the appearance energies of the various cations vary from 8.09 eV to 22.27 eV, whereas, the Wannier exponents range from 1.02 to 2.77. The appearance energy of the 1-butanol parent cation M^+ is 10.27eV, which is less than that of the corresponding parent cations in 1-propanol [54], methanol [52] and ethanol [52]. This observation indicates that the bigger molecules in the primary alcohol family need less energy to ionize an electron from the outermost valence orbital. The AE of the oxonium ion (31 amu), which is the most intense feature in the mass spectrum at 70 eV impact energy [58], is 11.76 eV. This value is very close to the values reported in NIST database of 11.36±0.06 or 11.46 eV. The AE of the oxonium cation, from electron impact ionization of 1-butanol, is somewhat higher than that previously observed for ethanol [52] and 1-propanol [54]. This reflects that more energy is required to remove an alkyl group from the longer molecular chain of the 1-butanol molecule, in order to form that oxonium cation. Two distinct AE thresholds at 10.36 eV and 13.21eV are observed for the cation fragment of mass 50 amu. Here the first AE is assigned to the $C_4H_2^+$ cation at 10.36 eV, while the second fragmentation onset at 13.21eV may be due to $C_4H_2^+$ formation from a background contaminant, as suggested by Feiegele *et al.* [66]. Here we note that $C_4H_2^+$ has a very low abundance (less than 1%), so it may indeed be susceptible to a contaminant.

For the cations with masses 53, 44, 41, 29 and 28 amu, we again find two values for the appearance energy in each case. This follows as each of these mass fragments could be formed through two distinct molecular fragments with identical mass value. For example, the m = 44 amu cation could originate from either $C_3H_8^+$ or $C_2H_4O^+$ fragments. As the production of each of these fragments proceeds through a different pathway, each fragment may have a distinct AE. Hence the observation of two unique AE thresholds. The 15 amu mass fragment also presents with two energy thresholds for its AEs, as was mentioned before in Section 2. In this case the CH_3^+ fragment may be produced through dipolar dissociation associated with dissociative ionization in the fragmentation process, as originally suggested by Böhler *et al*. [78]. Here each pathway has an energetic onset, which can present as a virtual AE. For the cations with mass 50 and 45 amu, multiple isomers of the single formula may be present to so produce two distinct values of the appearance energy [79]. For the mass cation m = 57 amu only a single AE is observed, suggesting that only one of the two possible $C_4H_9^+$ and $C_3H_5O^+$

cations is formed in the electron impact ionization of 1-butanol. Alternatively, one of these cations may have a rather short lifetime, and so undergo further fragmentation prior to being detected.

The cations with masses 40 - 43 amu have almost the same value for the appearance energy, and we note that all of these ions arise from the acetaldehyde cation $C_2H_4O^+$ with a sequential loss of H atoms. The C^+ cation (m=12 amu) has the highest appearance energy, primarily because each C atom is strongly bonded to the other carbon atoms and the hydrogen atoms. As such, sufficient energy and structural rearrangements are required to release a C^+ cation fragment.

The cations with masses of 54, 53, 52, 41, 29 and 15 amu all present with appearance energies below or close to the first ionization threshold. This observation is somewhat surprising as the ionization of the outermost orbital can form a stable parent cation. Analysis of the background signal indicates that the above fragments are related to 1-butanol. Ibănescu and Allan [80] have previously investigated dissociative electron attachment to primary alcohols, where they observed a prominent σ–Feshbach resonance in 1-butanol that can produce OH^-. This may occur though the following mechanism:

$$e\ (E_0 \sim 8.2eV) + C_4H_9OH \rightarrow OH^- + C_4H_7\ (54\ \text{amu}) + H_2.$$

Given the significant intensity of a resonance contribution to the total electron scattering cross section at impact energies close to this onset [81], this type of process, and similar, may produce a population of C_xH_y species that can then be singly ionized to produce weak ion signals within the present mass spectra at energies below the first ionization threshold of 1-butanol. Note that these fragments represent a particularly minor contribution to the present PICS [58], although they can be detected with the high ion sensitivity of the present apparatus, and the quite low energy resolution of the electron beam. The possibility of direct and sequential processes to produce a specific ion fragment could also explain the origin of two appearance energies for specific mass fragments, although we believe that the contribution of any sequential processes to our PICS is minor, particularly at larger impact energies where we have moved away from the dissociative resonances.

3.2 Total ionization cross sections

The absolute partial ionization cross sections (PICS) were measured for 38 cations of 1-butanol in the energy range 10-100 eV, as reported in our companion paper [58]. These 38 fragment cations account for 96.6 % of the total ion contributions to the mass spectra generated by electrons with impact energy 70 eV. The PICS of these 38 fragments were subsequently summed to give the 1-butanol TICS reported in table 2 and presented in figure 2. Here the PICS for fragments with masses of 1-2 amu, 17-24 amu, 65 amu, and 67-71 amu were not included in that sum to obtain the TICS, as those fragments either had a low abundance (making it difficult to obtain a PICS), were difficult to detect in the present spectrometer (H^+ and H_2^+) or had a high background that made it difficult to isolate the true PICS contribution from ionization of 1-butanol. Note again that the absolute scale of our TICS has been determined through a single point normalization of our data to that of Hudson *et al.* [44] at 70 eV, as described in the companion paper [58]. Hudson *et al.* [44] obtained absolute scale TICS values using an ionization cell, with the 70eV TICS value we employed being an interpolation from their actual measured data.

In figure 2, we also compare the present TICS to the experimental TICS data of Hudson *et al.* [44]. Our data is well matched with the Hudson data in the 55-100 eV energy range, whereas, it is larger in magnitude than the data of Hudson in the lower energy 10-50 eV range. We have previously observed this same characteristic TICS behavior for methanol [52], ethanol [52] and 1-propanol [54], when comparing between our TICS values and those of Hudson *et al.* [44] . This result suggests some systematic difference in the TICS obtained through the different techniques at lower energies. We now compare our experimental TICS data to the available theoretical data. The DM formalism result of Hudson *et al.* [44] agrees with the present experimental data in the low energy region, 10-30 eV, but then proceeds to overestimate all of the available experimental data in the higher energy region. This has also been observed for the other primary alcohols, and suggests a limitation with that approach.

There is some inconsistency amongst previously calculated BEB TICS cross sections available in the literature. Hudson *et al.* [44] originally calculated a BEB cross section and reported a maximum value of 11.90×10^{-20} m^2, which fell below their experimental maximum value of 12.85×10^{-20} m^2. Some of the same authors from ref. [44] recently reviewed ionization cross section calculation methods in Bull *et al.* [49], and obtained a maximum electron impact ionization cross section at the BEB level of 13.91×10^{-20} m^2. It is therefore important for us to independently check the implementation of the BEB cross section calculation. In our BEB implementation at the OVGF level, we achieve good agreement with the more recent BEB result from Bull *et al.* [49] that is performed at a similar level of approximation, although our calculation uses a smaller basis set. This provides independent verification that the BEB calculation of Bull *et al.* was implemented correctly [49], and so we only present our BEB values in figure 2 and not those from Bull *et al.* [49]. However, the data from Bull *et al.* is incorporated into our table 2. Our B3LYP BEB calculation is also in reasonable agreement with the OVGF BEB result, although they are typically 1-2% lower in magnitude. We therefore believe that the previous BEB result from Hudson *et al.*, also shown in figure 2, is erroneous as it underestimates the total ionization cross section of Hudson *et al.* at larger impact energies where the BEB formalism should work well. This is similar to what we previously observed in 1-propanol. The present BEB TICS gives good agreement with the experimental results, to within experimental uncertainty, up to energies of 50eV. At higher energies, the BEB calculation is somewhat larger in magnitude than the present experimental data, which may simply reflect that some of the PICSs are not included in obtaining the present TICS.

We have also calculated the total ionization cross section using our IAM-SCAR method, and those results are also presented within figure 2 and in table 2. Here we can see that there is reasonable agreement between the present IAM-SCAR and BEB calculations. The IAM-SCAR calculation gives a somewhat larger cross section than that obtained within the BEB formalism at energies between 30 and 60eV, but gives smaller values than the BEB as the incident electron energy increases toward 100eV. Within the IAM-SCAR formalism, the calculation may include contributions from other absorption channels, such as excitation and neutral dissociation, to produce a higher cross section than that seen at the BEB level. At larger impact energies, above 80eV, the IAM-SCAR TICS is in good agreement with the two sets of experimental values. This reflects the fact that the approximations employed within the IAM-SCAR formalism become more physical with increasing incident electron energy.

The correlation between the total ionization cross section and structural molecular properties, such as the dipole-polarizability, of the C1-C4 alcohols has previously been explored by Hudson *et al.* [44]. To build on that work, in figure 3 we present our TICS data for methanol [52], ethanol [52], 1-propanol [54] and 1-butanol, in the energy range 10-100 eV. From figure 3, we can clearly see that the TICS for the primary alcohols increases with the size

of the molecule, with 1-butanol having a larger TICS than the other three alcohols. The observed shapes of the TICS for the C1-C4 alcohols are also quite consistent for each molecule, over the threshold to 100 eV energy range. As Hudson *et al.* [44] have previously shown that the maximum intensity of the TICS can be described through a relationship between the molecular dipole-polarizability and the ionization threshold, the similar shape observed for the present C1-C4 alcohols suggests that the characteristic alcohol TICS shape might be rescaled, based on the empirical TICS maximum determined from a relevant dipole polarizability and ionization threshold, to approximate the TICS for larger alcohols whose cross sections are currently unknown.

4. Conclusions

Electron impact ionization of 1-butanol has been studied in the energy range 10-100 eV by employing a quadrupole mass spectrometer with a mass resolution of 1 amu. By summing the contribution of the PICS for the 38 main cation fragments [58], we have obtained the TICS for electron impact ionization of 1-butanol. Our TICS data are in good agreement with the only other available experimental result as measured by Hudson *et al.* [44] at energies above about 50 eV. While quite good agreement was typically observed with our BEB and IAM-SCAR calculated TICS values, the present data is not in agreement with TICS values calculated with the DM formalism from Hudson *et al.* [44]. This behavior was also observed previously by us with our TICS values of methanol [52], ethanol [52] and 1-propanol [54]. We have compared our present experimental TICS data of 1-butanol with our earlier TICS data of methanol, ethanol and 1-propanol, and shown that the TICS of the molecule increases in magnitude with the size of the primary alcohol. In addition, we have reported a comprehensive set of the appearance energies and Wannier exponents for 36 of the main cations fragments produced through electron impact ionization in 1-butanol, 32 of those cations fragments for the first time.

Acknowledgements

This work was supported by the Brazilian Conselho Nacional de Desenvolvimento Cientifico e Tecnológico (CNPq), Fundação de Amparo à Pesquisa do Estado de Minas Gerais (FAPEMIG) and FINEP. M.C.A.L., R.F.C.N. and H.V.D. acknowledge financial support from CNPq, while W.A.D.P., S. G. and R.A.A.A. acknowledge the fellowship from CAPES. KLN would like to thank CNPq for an 'Attracting Young Talent' fellowship. One of us (MJB) also acknowledges financial support from the Australian Research Council (DP160102787).

References

[1] J. H. Gross, Electron Ionization, in: Mass Spectrometry: A Textbook, Springer Berlin Heidelberg, Berlin, Heidelberg (2004)193-222.
[2] L. Campbell, M. J. Brunger, Int. Rev. Phys. Chem. **35** (2016) 297.
[3] M. A. Ridenti, J. A. Filho, M. J. Brunger, R. F. da Costa, M.T. do N. Verella, M. H. F. Bettega, M. A. P. Lima, Eur. Phys. J. D **70** (2016) 161.
[4] M. C. Fuss, L. Ellis-Gibbings, D. B. Jones, M. J. Brunger, F. Blanco, A. Muñoz, P. Limão-Vieira, G. Garcia, J. Appl. Phys. **117** (2015) 214701.
[5] M. J. Brunger, Int. Rev. Phys. Chem. **36** (2017) 333.

[6] A. K. Agarwal, Prog. Energy Combust. Sci. **33** (2007) 233.
[7] W. Fei, J. B. Liu, J. Sinibaldi, C. Brophy, A. Kuthi, C. Jiang, P. Ronney, M. A. Gundersen, IEEE T Plasma Sci **33** (2005) 844.
[8] D. E. Ramey, NABC Report **19** (2007) 137.
[9] S. Atsumi, T. Hanai, J. C. Liao, Nature **451** (2008) 86.
[10] N. Qureshi, B.C. Saha, B. Dien, R.E. Hector, M.A. Cotta, Biomass and Bioenergy **34** (2010) 559.
[11] N. F. Mott, Proc. R. Soc. London, Ser. A **124** (1929) 425.
[12] H. Bethe, Annalen der Physik **397** (1930) 325.
[13] M. Born, Z. Phys. **38** (1926) 803.
[14] Y.-K. Kim, M.E. Rudd, Phys. Rev. A **50** (1994) 3954.
[15] G. E. Scott, K. K. Irikura, Surf. Interface Anal. **37** (2005) 973.
[16] I. Plante, F. A. Cucinotta, Radiat. Prot. Dosim. **166** (2015) 19.
[17] H. Deutsch, K. Becker, R. Basner, M. Schmidt, T. D. Märk, J. Phys. Chem. A **102** (1998) 8819.
[18] M. Guerra, F. Parente, P. Indelicato, J. P. Santos, Int. J. Mass Spectrom. **313** (2012) 1.
[19] M. Guerra, P. Amaro, J. Machado, J. P. Santos, J. Phys.: Conf. Series **635** (2015) 052067.
[20] Y.-K. Kim, J. P. Santos, F. Parente, Phys. Rev. A **62** (2000) 052710.
[21] H. Tanaka, M. J. Brunger, L. Campbell, H. Kato, M. Hoshino, A. R. P. Rau, Rev. Mod. Phys. **88** (2016) 025004.
[22] D. Margreiter, H. Deutsch, M. Schmidt, T. D. Märk, Int. J. Mass Spectrom. Ion Processes **100** (1990) 157.
[23] M. Probst, H. Deutsch, K. Becker, T. D. Märkde, Int. J. Mass Spectrom. **206** (2001) 13.
[24] H. Deutsch, C. Cornelissen, L. Cespiva, V. Bonacic-Koutecky, D. Margreiter, T. D. Märk, Int. J. Mass Spectrom. Ion Processes **129** (1993) 43.
[25] H. Deutsch, T. D. Märk, V. Tarnovsky, K. Becker, C. Cornelissen, L. Cespiva, V. Bonacic-Koutecky, Int. J. Mass Spectrom. Ion Processes **137** (1994) 77.
[26] M. Vinodkumar, R. Dave, H. Bhutadia, B. Antony, Int. J. Mass Spectrom. **292** (2010) 7.
[27] R. Naghma, B. N. Mahato, M. Vinodkumar, B. Antony, Int. J. Mass Spectrom. **44** (2011) 105204.
[28] J. Kaur, D. Gupta, R. Naghma, D. Ghoshal, B. Antony, Can. J. Phys. **93** (2014) 617.
[29] H. Lüdde, A. Achenbach, T. Kalkbrenner, H.-C. Jankowiak, T. Kirchner, Eur. Phys. J. D **70** (2016) 82.
[30] D. B. Jones, R. F. da Costa, M. T. do N. Varella, M. H. F. Bettega, M. A. P. Lima, F. Blanco, G. García, M. J. Brunger, J. Chem. Phys. **144** (2016) 144303.
[31] F. Blanco and G. Garcia, J. Phys. B **42** (2009) 145203.
[32] O. Zatsarinny, K. Bartschat, G. Garcia, F. Blanco, L. R. Hargreaves, D. B. Jones, R. Murrie, J. R. Brunton, M. J. Brunger, M. Hoshino and S. J. Buckman, Phys. Rev. A **83** (2011) 042702.
[33] D. Rapp, P. Englander-Golden, J. Chem. Phys. **43** (1965) 1464.
[34] E. Krishnakumar, S. K. Srivastava, J. Phys. B: At. Mol. Opt. Phys. **21** (1988) 1055.
[35] O. J. Orient, S.K. Srivastava, J. Phys. B: At. Mol. Opt. Phys. **20** (1987) 3923.
[36] E. Krishnakumar, S.K. Srivastava, Int. J. Mass Spectrom. Ion Processes **113** (1992) 1.
[37] H. Nishimura, H. Tawara, J. Phys. B: At. Mol. Opt. Phys. **27** (1994) 2063.
[38] H. C. Straub, P. Renault, B. G. Lindsay, K. A. Smith, R. F. Stebbings, Phys. Rev. A **52** (1995) 1115.
[39] H. C. Straub, P. Renault, B. G. Lindsay, K. A. Smith, R. F. Stebbings, Phys. Rev. A **54** (1996) 2146.
[40] H. C. Straub, B. G. Lindsay, K. A. Smith, R. F. Stebbings, J. Chem. Phys. **108** (1998) 109.
[41] H. C. Straub, B. G. Lindsay, K. A. Smith, R. F. Stebbings, J. Chem. Phys. **105** (1996) 4015.

[42] S. K. Srivastava, E. Krishnakumar, A. F. Fucaloro, T. van Note, J. Geophys. Res. **101** (1996) 26155.
[43] R. Rejoub, C. D. Morton, B.G. Lindsay, R. F. Stebbings, J. Chem. Phys. **118** (2003) 1756.
[44] J. E. Hudson, M. L. Hamilton, C. Vallance, P. W. Harland, Phys. Chem. Chem. Phys. **5** (2003) 3162.
[45] S. Pal, Chem. Phys. **302** (2004) 119.
[46] M. Vinodkumar, K. Korot, P. C. Vinodkumar, Int. J. Mass Spectrom. **305** (2011) 26.
[47] K. M. Douglas, S. D. Price, J. Chem. Phys. **131** (2009) 224305.
[48] A. N. Zavilopulo, F. F. Chipev, L. M. Kokhtych, Nucl. Instrum. Methods Phys. Res., Sect. B **233** (2005) 302.
[49] J. N. Bull, P. W. Harland, C. Vallance, J. Phys. Chem. A **116** (2012) 767.
[50] T. Takeuchi, S. Ueno, M. Yamamoto, T. Matsushita, K. Nishimoto, Int. J. Mass Spectrom. Ion Processes **64** (1985) 33.
[51] D. G. M. Silva, T. Tejo, J. Muse, D. Romero, M. A. Khakoo and M. C. A. Lopes, J. Phys. B: At. Mol. Opt. Phys. **43** (2010) 015201.
[52] K. L. Nixon, W. A. D. Pires, R. F. C. Neves, H. V. Duque, D. B. Jones, M. J. Brunger, M. C. A. Lopes, Int. J. Mass Spectrom. **404** (2016) 48.
[53] D. G. M. Silva, M. Gomes, S. Ghosh, I. F. L. Silva, W. A. D. Pires ; D. Jones, F. Blanco, G. Garcia, S. J. Buckman, M. J. Brunger, M. C. A. Lopes, J. Chem. Phys. **147** (2017), 194307.
[54] W. A. D. Pires, K. L. Nixon, S. Ghosh, R. F. C. Neves, H. V. Duque, R. A. A. Amorim, D. B. Jones, F. Blanco, G. Garcia, M. J. Brunger, M. C. A. Lopes, Int. J. Mass Spectrom. **422** (2017) 32.
[55] R. A. Friedel, J. L. Shultz, A. G. Sharkey, Anal. Chem. **28** (1956) 926.
[56] P. Oßwald, H. Güldenberg, K. Kohse-Höinghaus, B. Yang, T. Yuan, F. Qi, Combust Flame **158** (2011) 2.
[57] B. W. Weber, C. -J. Sung, Energ. Fuel **27** (2013) 1688.
[58] W. A. D. Pires, K. L. Nixon, S. Ghosh, R. A. A. Amorim, R. F. C. Neves, H. V. Duque, D. G. M. da Silva, D. B. Jones, M. J. Brunger, M. C. A. Lopes, Int. J. Mass Spectrom. (2018), companion paper I.
[59] NIST Web Book :
http://webbook.nist.gov/cgi/inchi?ID=C71238&Mask=48Type=ANTOINE8Plot=on.
[60] J. Laskin, J. M. Behm, K. R. Lykke, C. Lifshitz, Chem. Phys. Lett. **252** (1996) 277.
[61] P. Scheier, B. Dünser, R. Wörgötter, M. Lezius, R. Robl, T. D. Märk, Int. J. Mass Spectrom. and Ion Proc. **138** (1994) 77.
[62] R. Wörgötter, B. Dünser, P. Scheier, T. D. Märk, J. Chem. Phys. **101** (1994) 8674.
[63] T. D. Märk, J. Chem. Phys. **63** (1975) 3731.
[64] G. H. Wannier, Phys. Rev. **90** (1953) 817.
[65] S. Matt, O. Echt, R. Wörgötter, V. Grill, P. Scheier, C. Lifshitz, T. D. Märk, Chem. Phys. Lett. **264** (1997) 149.
[66] T. Fiegele, G. Hanel, I. Torres, M. Lezius, T. D. Märk, J. Phys. B: At. Mol. Opt. Phys. **33** (2000) 4263.
[67] B. Gstir, S. Denifl, G. Hanel, M. Rümmele, T. Fiegele, P. Cicman, M. Stano, S. Matejcik, P. Scheier, K. Becker, A. Stamatovic, T. D. Märk, J. Phys. B: At. Mol. Opt. Phys. **35** (2002) 2993.
[68] S. Denifl, B. Sonnweber, G. Hanel, P. Scheier, T. D. Märk, Int. J. Mass Spectrom. **238** (2004) 47.
[69] A. R. Milosavljević, J. Kočišek, P. Papp, D. Kubala, B. P. Marinković, P. Mach, J. Urban, Š. Matejčík, J. Chem. Phys. **132** (2010) 104308.
[70] D. Wandschneider, M. Michalik, A. Heintz, J. Mol. Liq. **125** (2006) 2.
[71] R. D. Cowan, The Theory of Atomic Structure and Spectra, London: University of California Press, 1981.
[72] M. E. Riley, D. G. Truhlar, J. Chem. Phys. **63** (1975) 2182.

[73] X. Zhang, J. Sun, Y. Liu, J. Phys. B: At. Mol. Opt. Phys. **25** (1992) 1893.
[74] F. Blanco, G. García, Phys. Lett. A **295** (2002) 178.
[75] L. Chiari, A. Zecca, G. García, F. Blanco, M.J. Brunger, J. Phys. B: At. Mol. Opt. Phys. **46** (2013) 235202.
[76] F. Blanco, G. García, Chem. Phys. Lett. **635** (2015) 321.
[77] N.C. WebBook, http://webbook.nist.gov/cgi/cbook.cgi?ID=C71363&Mask=20.
[78] E. Bohler, J. Warneke, P. Swiderek, Chem. Soc. Rev. **42** (2013) 9219.
[79] L. A. Curtiss, D. J. Lucas, J. A. Pople, J. Chem. Phys. **102** (1995) 3292.
[80] B. C. Ibanescu, M. Allan, Phys. Chem. Chem. Phys. **11** (2009) 7640.
[81] M.H.F. Bettega, C. Winstead, V. McKoy, Phys. Rev. A **82** (2010) 062709.

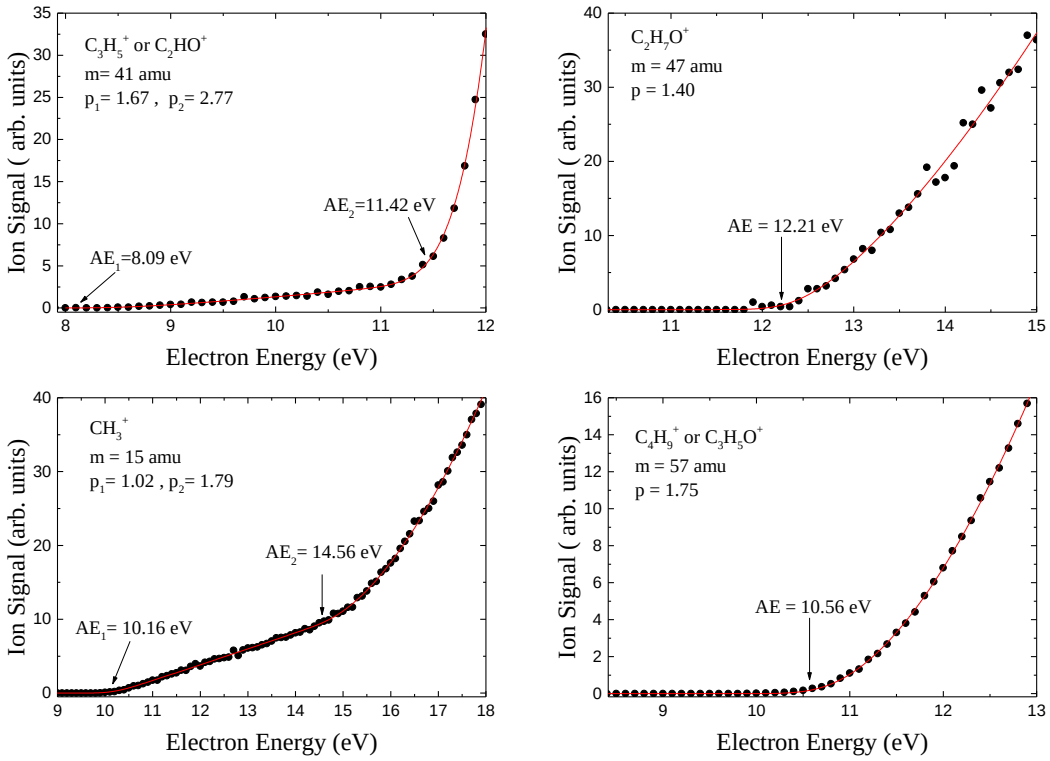

Figure 1: Results from the fitting procedure applied to determine the AEs from the experimental ionization efficiency curves, of specific ion fragments, produced through electron impact ionization of 1-butanol. The AEs are indicated by arrows, while the solid line shows the functions fitted to our experimental data for the cations of 15, 41, 47 and 57 amu. See text for further details.

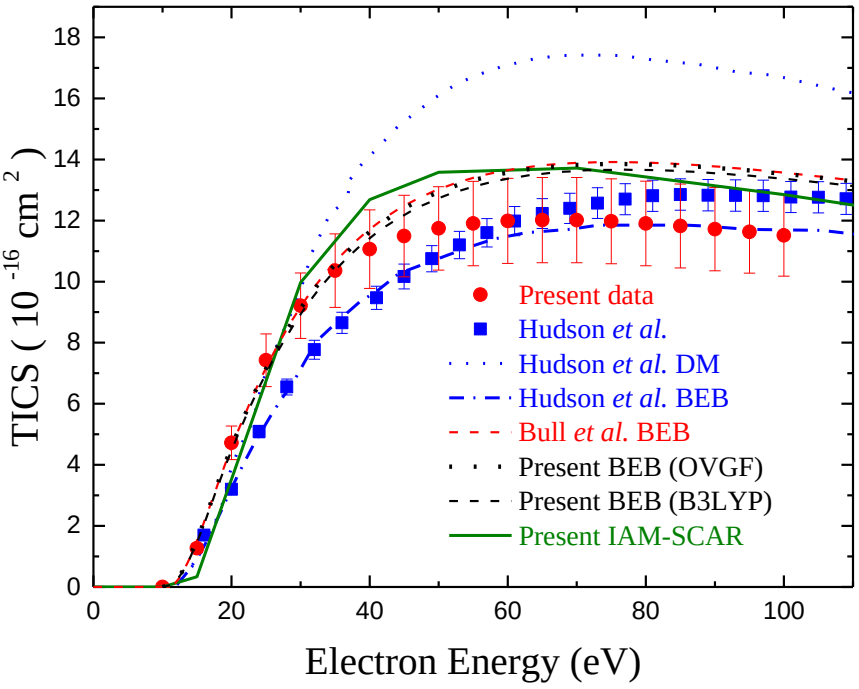

Figure 2: The electron impact total ionization cross section for 1-butanol obtained in this work. Our experimental data is also compared to our theoretical IAM-SCAR and BEB cross sections. Additionally shown are previously calculated DM and BEB cross sections [44] and a later BEB cross section [49], and the experimental data from Hudson *et al.* [44]. Our experimental TICS was obtained by taking into account the sum of 38 cations, representing 96.6% of the cations measured within the mass spectrum. See text and legend for further details.

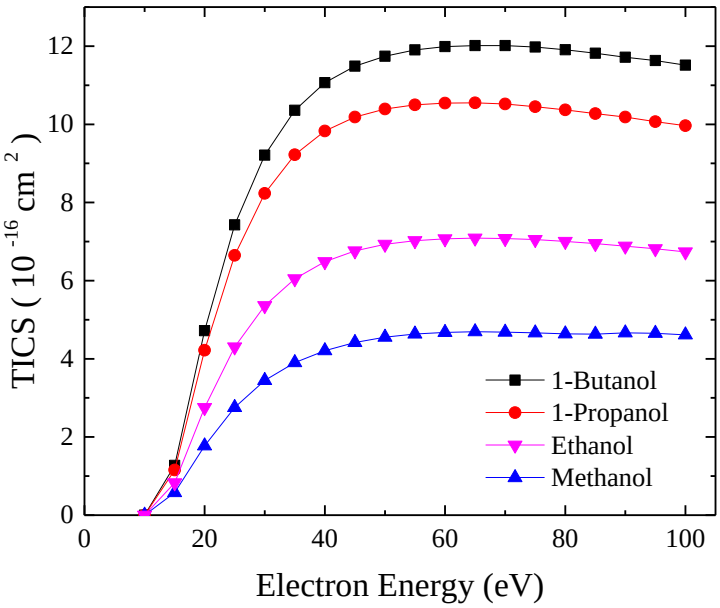

Figure 3: A comparison of the present electron impact total ionization cross sections of methanol, ethanol, 1-propanol and 1-butanol over the 10-100 eV energy range. Here the lines are shown as a guide only.

Table 1: Appearance energies (eV) and Wannier exponents, p, determined for 36 cations of 1-butanol formed during the fragmentation process by electron impact.

m (amu)	**NIST**[77]	**A.N. Zavilopulo**[48]	**Present Data**	**p**
74	10.10 ± 0.05[a] 9.99 ± 0.05[b] 10.64 ± 0.07[c] 10.09 ± 0.02[d] 10.37[e] [f]		10.27 ± 0.03	1.30 ± 0.02
73			11.14 ± 0.07	2.02 ± 0.12
72			10.12 ± 0.04	1.36 ± 0.03
60			10.93 ± 0.16	1.12 ± 0.14
59			11.24 ± 0.11	2.11 ± 0.14
58			10.72 ± 0.15	1.55 ± 0.12
57			10.56 ± 0.03	1.75 ± 0.03
56	10.18 ± 0.05[b] 10.20 ± 0.10[c]		10.48 ± 0.01	1.89 ± 0.02
55			11.61 ± 0.02	1.94 ± 0.02
54			9.63 ± 0.09	1.79 ± 0.10
53			9.91 ± 0.05	2.02 ± 0.10
			12.28 ± 0.28	1.32 ± 0.48
52			9.97 ± 0.09	1.49 ± 0.08
51			12.80 ± 0.18	1.95 ± 0.18
50			10.60 ± 0.13	1.80 ± 0.19
			13.12 ± 0.65	1.61 ± 0.70
47			12.21 ± 0.12	1.40 ± 0.10
46			11.30 ± 0.08	1.69 ± 0.08
45			11.72 ± 0.01	1.82 ± 0.15
			13.16 ± 0.20	1.52 ± 0.16
44			10.67 ± 0.02	1.65 ± 0.16
			12.11 ± 0.07	1.51 ± 0.04
43			11.65 ± 0.03	2.19 ± 0.04
42	11.23[g]		11.49 ± 0.03	1.89 ± 0.03
41			8.09 ± 0.46	1.67 ± 0.42
			11.42 ± 0.18	2.77 ± 0.60
40			11.52 ± 0.04	1.67 ± 0.05
39			10.71 ± 0.09	2.00 ± 0.08
38			13.25 ± 0.30	1.82 ± 0.26
37			16.26 ± 0.55	2.59 ± 0.26
33			11.60 ± 0.01	1.59 ± 0.01
32			11.09 ± 0.03	1.71 ± 0.03
31	11.36 ± 0.06[h] 11.46[g]	11.82	11.76 ± 0.02	2.00 ± 0.02
30			11.08 ± 0.11	1.65 ± 0.15
29			8.91 ± 0.13	1.62 ± 0.07
			12.57 ± 0.10	2.59 ± 0.14
28			10.94 ± 0.03	1.50 ± 0.27
			12.34 ± 0.11	1.78 ± 0.13
27			13.63 ± 0.05	2.68 ± 0.06
26			11.60 ± 0.07	1.44 ± 0.02
15			10.16 ± 013	1.02 ± 0.07
			14.56 ± 0.10	1.79 ± 0.03
14			15.27 ± 0.12	1.52 ± 0.10
12			22.27 ± 0.15	1.51 ± 0.07

(a) Holmes, J.L., Lossing, F.P., Org. Mass Spectrom. **26** (1991) 537.

(b) Shao, J.D., Baer, T., Lewis, D.K., J. Phys. Chem. **92** (1988) 5123.

(c) Bowen, R.D., Maccoll, A., Org. Mass Spectrom. **19** (1984) 379.

(d) Cocksey, B.J., Eland, J.H.D., Danby, C.J., J. Chem. Soc. **(B)** (1971) 790.

(e) Baker, A.D., Betteridge, D., Kemp, N.R., Kirby, R.E., Anal. Chem. **43** (1971) 375.

(f) Katsumata, S., Iwai, T., Kimura, K., Bull. Chem. Soc. Jpn. **46** (1973) 3391.

(g) Lambdin, W.J., Tuffly, B.L., Yarborough, V.A., Appl. Spectry. **13** (1959) 71.

(h) Selim, E.T.M., Helal, A.I., Indian J. Pure Appl. Phys. **19** (1981) 977.

Table 2: The present experimental and theoretical BEB and IAM-SCAR total ionization cross sections (10^{-16} cm^2) for electron impact on 1- butanol. Also shown are corresponding BEB results from Bull *et al.* [49]. Errors on the present experimental TICS are ~11.6% at each energy. See text for further details.

Energy (eV)	**Present BEB(OVGF)**	**Present BEB(B3LYP)**	**Present IAM-SCAR**	**TICS BEB** **Bull *et al.***	**Present TICS (experimental)** (11.6%)
10	0.00	0.00	0.00	0.00	2.2×10^{-4}
15	1.54	1.47	0.33	1.50	1.27
20	4.58	4.47	3.53	4.57	4.72
25	7.15	6.99		7.18	7.43
30	9.12	8.93	9.97	9.18	9.21
35	10.57	10.37		10.64	10.36
40	11.63	11.42	12.68	11.71	11.06
45	12.40	12.18		12.48	11.49
50	12.94	12.73	13.58	13.02	11.74
55	13.32	13.11		13.40	11.90
60	13.57	13.37		13.65	11.99
65	13.73	13.53		13.80	12.01
70	13.82	13.63	13.72	13.89	12.01
75	13.85	13.66		13.91	11.98
80	13.84	13.66		13.90	11.91
85	13.80	13.62		13.85	11.82
90	13.73	13.55		13.77	11.72
95	13.64	13.47		13.68	11.63
100	13.53	13.37	12.85	13.57	11.51